Superradiance and Exciton Delocalization in Bacterial Photosynthetic Light-Harvesting Systems

René Monshouwer,* Malin Abrahamsson, Frank van Mourik, and Rienk van Grondelle

Department of Biophysics, Faculty of Physics and Astronomy, Vrije Universiteit, De Boelelaan 1081, 1081 HV Amsterdam, The Netherlands

Received: October 29, 1996; In Final Form: April 22, 1997[⊗]

We present temperature-dependent fluorescence quantum yield and lifetime measurements on the LH-1 and LH-2 complexes of *Rhodobacter sphaeroides* and on the isolated B820 subunit of *Rhodospirillum rubrum*. From these measurements the superradiance is calculated, which is related to the delocalization of excitations in these complexes. In the B820 preparation we find a radiative rate that is 30% higher than that of monomeric bacteriochlorophyll, in agreement with a dimer model of this subunit. At room temperature both LH-1 and LH-2 are superradiant relative to monomeric Bchl-*a* with enhancement factors of 3.8 and 2.8, respectively. In LH-2 the radiative rate does not change significantly upon lowering the temperature to 4 K. LH-1 however exhibits a strong temperature dependence, giving rise to a 2.4 times higher radiative rate at 4 K relative to room temperature. From modeling of the superradiance using a Hamiltonian based on the LH-2 structure and including site inhomogeneity, we conclude that the ratio of inhomogeneity over the coupling between the pigments is around 1 for LH-1 and 2−3 for LH-2. From the Monte Carlo simulations we estimate the delocalization length in LH-1 and LH-2 to be on the order of 3−4 pigments at room temperature.

I. Introduction

Primary processes in photosynthesis are the absorption of light and the subsequent transportation of excited-state energy to the reaction center. In the reaction center, the excited-state energy is used to create a charge separation that drives subsequent biochemical processes that convert the electronic energy into chemical energy.[1,2] In purple bacteria the so called LH-1 or core antenna complex is present in a fixed stoichiometry to the reaction center and is assumed to be closely associated with it. Some species have an additional type of antenna complex, LH-2, which is present in variable amounts and is thought to be more on the periphery of the photosynthetic apparatus. Recently the high-resolution X-ray structure of the LH-2 complex of *Rhodopseudomonas acidophila* has been published,[3,4] which has contributed to our insight into the structural organization of the pigments in these antenna complexes. The publication of the high-resolution structure of the LH-2 complex of a related bacterium (*Rhodospirillum molischianum*)[5] and the low-resolution electron micrographs of the LH-1 antenna of *Rhodospirillum rubrum*[6] indicates that the arrangement of two concentric rings of transmembrane α and β helixes with the pigments packed between them is a universal motif in these antenna systems. The pigments in the LH-2 complex can be subdivided in two groups, the B800 and B850 pigments. The B800 pigments are relatively far apart (21.2 Å) and are considered to be monomeric. The 18 pigments in the B850 band are very close together, 8.9 and 9.6 Å inter- and intraprotomer distance, respectively.[3,4] The strong electronic coupling that results from the close packing of the pigments suggests that exciton interaction is important in these antenna complexes. Using the structural parameters from the X-ray structure, several groups have modeled the excitonic behavior of these ringlike structures.[7−11] In most studies however, no site inhomogeneity of the pigments, nor electron−phonon coupling, was incorporated in the modeling. As was shown by Leegwater,[12] interaction of the pigments with phonons can strongly diminish the degree of exciton delocalization in the complex. Moreover, it has been shown that the absorption bands of these pigment−protein complexes are inhomogeneously broadened; i.e., due to small differences in the environment, each pigment has a slightly different absorption maximum.[13−17] This effect causes a decrease in exciton delocalization and significant changes in the spectroscopic properties of these complexes.

A spectroscopic observable that is directly related to the exciton delocalization is the so-called superradiance. This term means that the radiative rate of a complex of pigments is larger than that of the individual pigments. This phenomenon has been observed in strongly coupled molecular aggregates and has been taken to reflect collective behavior of the pigments within the aggregate. The structure of the LH-2 antenna shows a similarity to these molecular aggregates in the sense that also these aggregates consist of an array of strongly coupled pigments. Well-known molecular aggregates of pigment molecules are the so called J-aggregates, which are linear chains of dye molecules such as pseudo-isocyanine or related pigments. It has been known since 1936[18,19] that aggregation of these dye molecules has a dramatic effect on the spectroscopic properties of these complexes. After aggregation a narrow and intense, red-shifted absorption band occurs, which is called the J-band. The width of this band is much narrower than that of the original monomer absorption. Furthermore, the fluorescence rate and quantum yield of these complexes are significantly enlarged, in particular at low temperatures. These spectroscopic changes have been ascribed to strong dipole−dipole coupling between the pigment molecules in the aggregate which delocalizes the excitation over part of the chain. Introduction of disorder and electron-phonon coupling has given a satisfactory description of the linear and nonlinear spectroscopy of J-aggregates.[20,21] Even though it is tempting to compare the photophysical properties of bacterial antenna complexes with those of molecular J-aggregates, there are some large differences between them. First, the pigment organization is much different. In the antenna complex, the aggregation size is small (18 pigments in the B850 pool of the LH-2 antenna of *Rps. acidophila*, and probably 32 pigments in

[⊗] Abstract published in *Advance ACS Abstracts,* August 15, 1997.

S1089-5647(96)03377-9 CCC: $14.00

LH-1) and the organization is not linear but in a ring. Especially the last feature has large influence on the spectroscopic properties of the exciton bands since the symmetry makes the lowest transition (which is the intense J-band in the case of linear aggregates) optically forbidden. Furthermore, the pigments in the bacterial complex are alternatingly ligated to histidines in the transmembrane part of the α or β polypeptide, respectively. It is known that the ligation influences the spectroscopic properties of the pigments, as for instance the site energy of the chromophores. Additional specific interactions are present like hydrogen bonding or the close presence of aromatic residues. These interactions can shift the central absorption of the pigments away from the wavelength of absorption in solution. Apart from these, several other parameters that determine the electronic properties and interactions between the pigments are different. The dipole−dipole coupling is for instance stronger in J-aggregates, whereas the disorder in bacterial antenna complexes is probably much larger (vide infra). Both effects can markedly affect the spectroscopic properties of these complexes.

In this paper we present measurements of the superradiance of different bacterial antenna complexes. Furthermore we have performed Monte Carlo simulations of the spectral properties of ringlike pigment arrays including both excitonic interaction and static inhomogeneity. Due to the symmetry of the ring, the lowest exciton state of a homogeneous ring is almost dipole forbidden. However, for a ring of 18 pigments, inhomogeneity causes an increase of the dipole strength of the lowest state to a maximum of 3.2 times the monomer. Furthermore our simulations show that even a moderate degree of inhomogeneity causes localization of the exciton on 3−4 pigments in LH-2.

II. Materials and Methods

The LH-1 and LH-2 samples of *Rhodobacter sphaeroides* were prepared as described before.[22,23] The B820 samples were prepared as described in ref 24 except that in this preparation an extra purification step on a Superdex 200 gel filtration column was added to ensure that no reaction centers were present. Bchl-*a* was purchased from Sigma and dissolved in acetone. The samples were immersed in a potassium buffer (pH 7.8) with a detergent concentration of 1.15% OGP for B820, 1% OGP for LH-1, and 0.1% LDAO for LH-2. For low-temperature measurements the samples were diluted in a buffer containing more than 70% v/v glycerol to ensure a transparent sample at low temperatures. Fluorescence spectra were measured using a $^1/_2$ m polychromator in combination with a cooled CCD camera. The sample was excited by a CW Ti-sapphire laser. The intensity of the excitation light was kept below 100 μW/cm^2. The fluorescence was detected under magic angle, to cancel any effects of depolarization on the fluorescence. Fluorescence lifetimes were measured using a Hamamatsu C5680-24 synchroscan streak camera with a time resolution of approximately 20 ps. The sample was excited at a repetition rate of 200 kHz using a femtosecond laser system as described in ref 25. The excitation density was kept low ($<$80 μW/cm^2) to prevent any photodamage or annihilation. The fluorescence was detected under magic angle. Room temperature relative fluorescence quantum yields were calculated by correcting for the wavelength dependence sensitivity of the spectrograph and subsequently integrating the fluorescence spectra on a wavenumber scale and normalizing them to the number of absorbed photons calculated from the OD of the sample at the excitation wavelength. The wavelength dependence of the fluorescence spectrograph was determined by comparing the emission of a standard tungsten lamp with the emission profile specified by the factory.

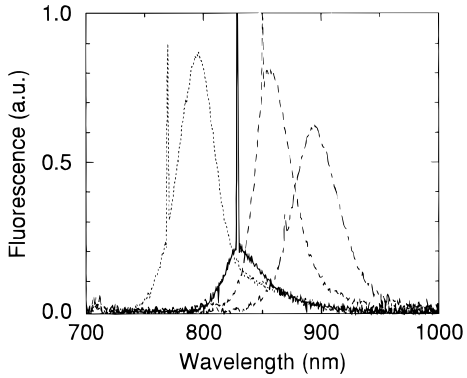

Figure 1. Room temperature fluorescence emission spectra of the different antenna complexes studied. The spectra were corrected for the wavelength-dependent sensitivity of the detector and normalized on the amount of absorbed photons. Shown are the emission spectra of Bchl-*a* in acetone (dotted, λ_{exc} = 770 nm), B820 of *Rs. rubrum* (solid, λ_{exc} = 830 nm), and LH-2 (dashed, λ_{exc} = 850 nm) and LH-1 (dash−dot, λ_{exc} = 870 nm) of *Rb. sphaeroides*.

TABLE 1: Fluorescence Quantum Yields and Fluorescence Lifetimes of Bchl-*a* in Acetone, the B820 Subunit of *Rs. Rubrum*, and the LH-1 and LH-2 Complexes of *Rb. Sphaeroides* at Room Temperature

	fluorescence quantum yield (%)	fluorescence lifetime (ps)	radiative lifetime (ns)	ϵ_r	emitting dipole strength
Bchl-*a*	18[b]	3140[b]	16.6	1.85	1.0
B820	3	590	19.7	2.3	1.3
LH-2	9.86	986	10	2.3	2.8
LH-1	8.14	680	8.4	2.3	3.8

[a] The quantum yields were measured relative to Bchl-*a* in acetone and normalized to the quantum yield from literature.[26] The radiative lifetimes were calculated using the relation $\tau_{rad} = \tau_{fl}/\phi_{fl}$. The emitting dipole strength was calculated using eq 1, taking the relative dielectric constants tabulated and using n = 1.36 and n = 1.33 for acetone and water, respectively. [b] Values taken from Connolly et al.[26]

III. Results

In Figure 1 the room temperature emission spectra of Bchl-*a* in acetone, B820, LH-2, and LH-1 are shown, normalized on the number of absorbed photons. It is clear from the LH-2 spectrum that the fluorescence from this complex is dominated by emission from the B850 pigments. The quantum yields derived from these emission spectra are listed in Table 1. To estimate the absolute fluorescence quantum yield, we have calibrated all measured (relative) quantum yields to the value determined for Bchl-*a* in acetone.[26] Listed in Table 1 are also the measured fluorescence lifetimes of the same samples at room temperature. The decay of the fluorescence was monoexponential, and the lifetimes agree well with previous measurements by others.[23,27] In the course of the experiments, it was noted that the lifetime and fluorescence quantum yield of the LH-1 sample were strongly dependent on the aggregation state of the sample, i.e., the number of LH-1 rings that can transfer excitations to each other. In membrane fragments of M2192 for instance a very short (~300 ps) decay of the fluorescence was found. The dependence of the fluorescence lifetime on the aggregation state was previously observed in pump probe measurements and was ascribed to trapping of the excitation by impurities.[23] Even though the extra nonradiative decay channel does not influence the calculation of the radiative rate, we have performed our measurements on a sample with minimal aggregation (see ref 23 for details). Furthermore, both lifetime and fluorescence quantum yield measurements were performed on the same sample.

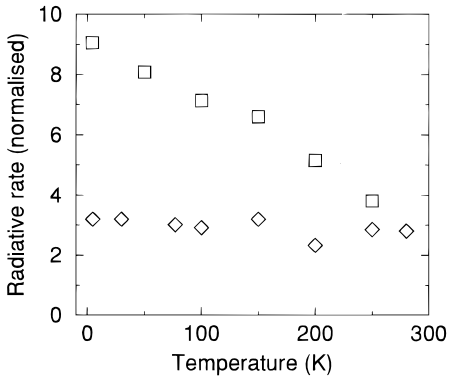

Figure 2. Temperature dependence of the radiative rate of LH-1 (squares) and LH-2 (diamonds) of *Rb. sphaeroides*. The temperature dependence was obtained by measuring both the temperature dependence of the fluorescence quantum yield (ϕ_{fl}(T)) and the fluorescence lifetime ($\tau_{fl}(T)$). From this the temperature-dependent radiative rate was calculated using the relation $k_{rad}(T) = \phi_{fl}(T)/\tau_{fl}(T)$. The absolute value was determined by normalizing the radiative rate to the values obtained at room temperature (see Table 1).

From the quantum yield and the fluorescence lifetime, the radiative rate (k_{rad}) can be calculated using the following relation: $k_{rad} = \phi_f/\tau_{fl}$. This rate can subsequently be related to the dipole strength of the emitting state using the formula of the Einstein coefficient for spontaneous emission:[28]

$$k_{rad} = A_{21} = \frac{16\pi^3}{3\epsilon_0 hc^3}\left[\frac{n^3}{\epsilon_r}\right]\nu^3|\mu|^2 \qquad (1)$$

In eq 1, the refractive index n is of the bulk solution, whereas the relative dielectric constant ϵ_r is of the direct surroundings of the chromophore, the protein. For all samples, the refractive index of the bulk (water or acetone) is almost identical (1.33 and 1.36, respectively). For Bchl-*a* in acetone, the refractive index of the direct surroundings is identical with the bulk, so $\epsilon_r = n^2 = 1.85$. Using the radiative lifetime from Connolly et al.,[26] we calculate using eq 1 a (vacuum) dipole strength of 68 D^2 for Bchl-*a* in acetone.[29] In case of the antenna complexes, the relative dielectric constant of the protein is essentially not known. This poses a problem in the comparison between the monomeric Bchl-*a* and the protein-bound pigments. Several authors have studied the local environment of protein-bound pigments by comparing the in vivo properties of these pigments with the pigments in different solvents. From this Renge et al.[30] estimated a refractive index of 1.51 for the protein surrounding the β-carotenoid in CP47 at room temperature. Using the same method Andersson et al.[31] estimated a refractive index of 1.63 for the protein surrounding the sphaeroidene in the LH-2 complex of *Rb. sphaeroides*. However, from the X-ray structure of *Rps. acidophila* it is known that there is very close contact between the carotenoid and one of the Bchl-*a* molecules of the B850 pigment pool. This could have slightly influenced the estimated refractive index in the LH-2 complex. In Table 1 we have added the relative dipole strengths of the emitting dipoles calculated using eq 1 and taking $\epsilon_r = 2.3$ for the antenna complexes (see Discussion).

Figure 2 shows the temperature dependence of the radiative rate calculated from the experiments. In LH-2 the temperature dependence of both the quantum yield and the fluorescence lifetime is quite weak. The fluorescence lifetime increases from about 1 to 1.25 ns whereas the quantum yield of fluorescence increases about 40% upon cooling down from room temperature to 4 K. The radiative rate of LH-2 calculated from these measurements is fairly constant; there is a slight (~15%) increase of the emitting dipole strength with decreasing temperature. However for LH-1 the increase of the radiative rate upon lowering the temperature is much more dramatic. The quantum yield of fluorescence increases with about a factor of 3.6 upon cooling down from 250 to 4 K. The fluorescence lifetime increases in the same temperature range from 535 to 821 ps, resulting in an increase of the radiative rate at 4 K to 2.35 times the value at room temperature. The somewhat lower room temperature fluorescence decay time suggests that the sample is slightly aggregated in glycerol, which is known to cause a shortening of the lifetime due to additional quenching processes (see above). However, we note that the lifetimes and quantum yields were obtained from the same sample, and thus the calculated radiative lifetime is independent of this extra quenching process. To correctly calculate the true dipole strength of the emitting state the temperature dependence of the refractive index contributions to eq 1 needs to be known. To estimate these we have measured the temperature-dependent absorption spectra of both LH-1 and LH-2 and determined the integrated absorption intensity of the B880 and B850 bands, respectively. The absorption spectra of both complexes show a slight (~10%) increase of the dipole strength upon cooling. If we assume that this is caused by a change in the dielectric constant of the protein, this could lead to a slight overestimation of the oscillator strength at low temperatures (see Discussion).

Monte Carlo Simulations. To calculate the average strength of the emitting dipole in LH-2 and LH-1 of *Rb. sphaeroides*, we have performed a Monte Carlo simulation of the spectral properties of inhomogeneously broadened circular pigment arrays. The method used is essentially identical with that used by Fidder et al. and Jimenez et al.[21,32] In short, for each Monte Carlo iteration an interaction matrix was generated with the site energies of the pigments on the diagonal and the coupling energies between the pigments (V) off diagonal. The site energies were randomly taken from a Gaussian distribution with fwhm σ_{inh}. The interactions between the pigments were fixed (so no dependence on the actual site energies), and only nearest-neighbor interactions were incorporated. The latter is justified by the large (R^3) distance dependence of the dipole−dipole interaction. This interaction matrix was diagonalized numerically,[33] and the eigenvectors and eigenvalues were used to calculate the energies and dipole strengths of the exciton levels.[34] Typically around 10 000 iterations were made. The positions and orientations of the pigments were taken from the 9-fold symmetrical structure of the LH-2 complex of *Rps. acidophila*.[3] For the LH-1 simulations, we have based the structure on the electron microscopy work by Karrasch et al.[6] and simply enlarged the LH-2 structure to accommodate 32 pigments.

To calculate the effective emitting dipole strength at low temperature ($k_bT \ll V$), we assume that the excitation relaxes to the lowest exciton state of the exciton manifold on a time scale much faster than the fluorescence lifetime. In that case the dipole strength of the emitting state is simply that of the lowest level in the exciton manifold. In Figure 3 we have plotted the dipole strength of the lowest state versus the inhomogeneity for different sizes of the ring. The curve with $N = 18$ models the LH-2 complex of *Rps. acidophila*, whereas 32 is the estimated number of pigments in LH-1.[6] At $\sigma_{inh} = 0$, the exciton levels can be calculated analytically, and the lowest exciton state is the so called $k = 0$ state of the exciton manifold.[7,20,32,35] The intensity of this state is close to zero since the "out of plane" intensities of the dipoles are small and moreover largely cancel due to the opposite perpendicular components of the α and β Bchl-*a* pigments.[3,4] Increasing the inhomogeneity causes a rapid increase of the dipole strength.

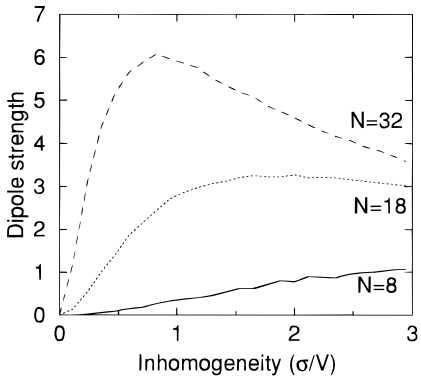

Figure 3. Dependence of the dipole strength of the lowest state of the exciton manifold on the amount of inhomogeneity for different ring sizes. The coupling between all neighboring pigments is V, and the orientation of the dipole moments within the protomer was taken from the crystal structure of *Rps. acidophila*.[3,4] The dipole strength is given in units of the monomer dipole strength. The inhomogeneity, σ, is the fwhm of the inhomogeneous distribution function of the monomer transitions.

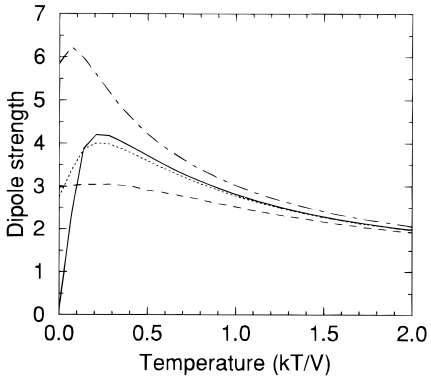

Figure 4. Temperature dependence of the emitting dipole strength for different values of σ/V. The temperature dependence for a ring of 18 pigments is shown for $\sigma/V = 0$ (solid), $\sigma/V = 1$ (dotted), and $\sigma/V = 3$ (dashed). For a ring of 32 pigments, the temperature dependence is shown for $\sigma/V = 1$ (dash−dot).

The reason for this is that the disorder disturbs the delicate "cancelling" of the dipole strength of the $k = 0$ state. In other words, symmetry breaking due to the disorder causes mixing of the $k = 0$ with the $k \pm 1$ states, which makes this lowest state allowed and polarized in the ring. Note however that, due to the disorder, the "k" states defined in the homogeneous case lose their identity. For higher inhomogeneities, the dipole strength of the lowest state decreases again since the static disorder creates a breakdown of the exciton delocalization. For $\sigma_{\text{inh}} \rightarrow \infty$, the exciton states converge to the monomeric states, and the dipole strength accordingly goes to 1. For a ring consisting of 18 monomers, like the LH-2 complex of *Rps. acidophila*, this shows that, independent of the coupling strength, the maximum emitting dipole strength at 4 K is about 3.2 times that of the monomer. At higher temperatures, the excitation will be distributed over the exciton manifold according to a Boltzmann distribution. To calculate the effective emitting dipole strength as a function of temperature, we have averaged the dipole strengths of all transitions, weighted with the Boltzmann population probability of each level. The result is shown in Figure 4 where the temperature dependence for a ring consisting of 18 pigments with different degrees of inhomogeneity is shown. At $k_bT \ll V$ the values are equal to those in Figure 3. Raising the temperature causes thermal population of the higher lying exciton states, which in general have more dipole strength. This causes the initial increase of dipole strength. At even higher temperatures, the population will be more evenly distributed over the whole exciton manifold, and for $T \rightarrow \infty$, the average emitting dipole strength will converge to 1. For $\sigma_{\text{inh}} = 0$ the temperature dependence is very pronounced, especially between 0 and 100 K. If however the lowest exciton state is partially allowed due to disorder the dependence is quite weak. The maximum increase in superradiance at higher temperatures is limited to about 4.2 for a ring of 18 pigments. For a ring consisting of 32 pigments, the maximum enhancement is 7.6.

Localization. A point of extensive discussion is the so-called exciton delocalization length within the antenna complex.[2] Several definitions of this term have been used in the discussions about exciton delocalization. For instance, Pullerits et al.[8] and Koolhaas et al.[10] estimated the amount of exciton delocalization by taking the minimum number of pigments required to mimic some of the observed spectral properties of the LH-2 complex. Other authors[12,32,36] have looked at the so-called inverse participation ratio that is defined by:[21,37]

$$R(E) = \frac{1}{N_{\text{coh}}(E)} = \frac{1}{N}\left\langle \sum_i \delta(E - E_i) \sum_j a_{ij}^4 \right\rangle / \rho(E) \qquad (2)$$

where a_{ij} is the ith element of the eigenvector belonging to the exciton state j and the angular brackets indicate the Monte Carlo averaging. Within this definition, $N_{\text{coh}}(E)$ is the average number of coherent pigments of the states at energy E. Note that N_{coh} of a strongly coupled system without inhomogeneity is not per definition 18 (as stated by Jimenez et al.[32]). For a ring, for instance, N_{coh} is 18 for the forbidden $k = 0$ and $k = 9$ transitions but equal to 12 for all other states (that contain the oscillator strength). To quantitatively look at the differences between these methods and the relation of the estimated N_{coh} to the exciton states, we have calculated the actual "average squared wave function" of the states that have significant dipole strength. The ith component of the vector belonging to the jth exciton state, $|a_{ij}|^2$, is a measure of the contribution of this pigment to the jth exciton state. A plot of this vector thus gives an indication of the distribution of the pigments that participate in the exciton state. To accumulate this distribution in our Monte Carlo scheme, we have, for each exciton state, averaged the squared eigenvectors, weighed with the dipole strength of the exciton state. Therefore we mainly look at the transitions that contribute to the spectroscopic properties. Since the center of the eigenfunction changes from state to state, we located the center of weight of each state and used this center to "align" all the vectors before averaging them. The result of this is shown in Figure 5, where averaged eigenvectors are shown for the cases $\sigma_{\text{inh}}/V = 0.1$, 1, and 3. The eigenvector belonging to $\sigma_{\text{inh}}/V = 0.1$ is close to the analytical solution for the completely delocalized $k \pm 1$ state.[21,32] These functions are cosine like functions with frequency $2\pi/N$, where N is the number of pigments in the ring. For larger inhomogeneity it is clear that the occupancy is more and more located around the center of weight of each eigenfunction. This process visualizes the concept of localization. For $\sigma_{\text{inh}}/V \rightarrow \infty$ only the central pigment has nonzero excitation density, and thus each "exciton" state is identical to one of the monomer states. Any definition of "delocalization length" is a statistical estimate of the width of the distribution. In case of $\sigma_{\text{inh}}/V = 1$, we find for the participation ratio a value of 8.3, the second moment of the distribution is 5.4, and the fwhm is 2.6 pigments. From this comparison it is clear that the delocalization length found is very dependent on the definition of the term. Even though the number depends on the definition, it is obvious that the

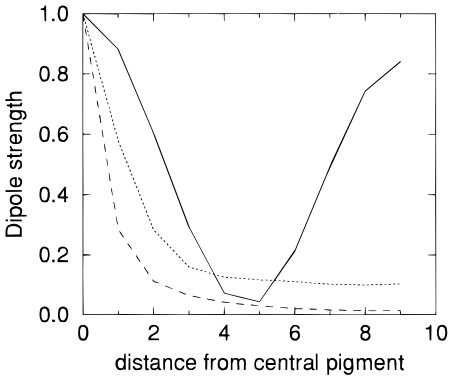

Figure 5. Shape of the delocalization of the exciton for different amounts of inhomogeneity for a ring of 18 pigments. Shown is the average contribution of pigment i to exciton state k, $|a_{ij}|$, as a function of the distance of this pigment to the center of weight of the exciton distribution. The distributions shown are normalized to 1 for the central pigment and weighed with the dipole strength of the exciton transition, $|\mu_j|^2$. The solid line is for $\sigma/V = 0$, dotted is $\sigma/V = 1$, and dashed is $\sigma/V = 3$.

differences are very large, and care should be taken when comparing the individual results. In the extreme case of infinite inhomogeneity all three methods yield the same result, namely 1.

IV. Discussion

Excitons and Disorder. Following the resolution of the structure of the LH-2 complex of *Rps. acidophila*,[3,4] revealing the B850 pool as a tightly packed circular array of Bchl molecules, a lively debate has started concerning the nature of the excited state.[2] On one hand the excited state is considered as essentially delocalized over the whole ring (fully delocalized exciton model), while on the other hand the excitation is taken to be essentially localized on one or only a few molecules. In this work we have studied one observable that is indicative of exciton delocalization, the so-called superradiance. Superradiance is the increase of the radiative rate caused by the effect that, in an exciton manifold, one specific exciton transition can gather much more dipole strength than that of the monomer. Since the dipole strength is directly related to the radiative rate (see eq 1), this can cause a strong increase of the observed rate. For instance, in the linear J-aggregates, an increase of the radiative rate of more than a factor of 100 has been observed.[38] In case of a ringlike organization of the pigments, the result of a calculation of the radiative enhancement is different from that of J-aggregates. The exciton spectrum of a ring like the B850 band of the LH-2 complex without inhomogeneity consists of 16 doubly degenerate transitions and 2 nondegenerate transitions, spanning an exciton band with a width of four times the coupling strength between the pigments. The lowest transition of the exciton manifold ($k = 0$) has a dipole strength close to zero and is polarized perpendicular to the plane of the ring. The two next (lowest degenerate) transitions carry almost all the dipole strength and are polarized in the plane of the ring. These properties differ strongly from those of the J-aggregates where the lowest transition carries almost all the dipole strength. Sauer et al.[11] and Sturgis et al.[9] have shown that it is possible to calculate the red-shift of the linear absorption spectrum of the LH-2 complex with such a ringlike and fully delocalized exciton model. However experimental evidence is in contradiction with a model where the lowest transition is forbidden and perpendicular to the plane of the ring. From fluorescence quantum-yield (this paper) and polarized fluorescence measurements, it is known that, even at 4 K, the emission from the LH-2 antenna has not significantly decreased compared to that at room temperature and furthermore is polarized in the plane of the ring.[32,39,40] Consequently, the model used by Sauer et al. and Sturgis et al. is a large oversimplification of the spectroscopy of such an antenna complex. In addition to the interactions between the pigments, each pigment also interacts and couples to the environment (the protein). Site-directed mutagenesis of the LH-2 antenna of *Rb. sphaeroides* has for instance shown that the absorption of the B850 band can be shifted by changing a single amino acid in the vicinity of the pigments.[41] Apart from distinctly different binding pockets of the pigments (as for instance the binding site of the B800 and the α and β B850 Bchl-*a* pigments in the LH-2 complex) there are also (random) fluctuations of the environment that influence the absorption of the pigments. If the fluctuations are static (i.e., fluctuating on a time scale longer than the coherence time of the pigments), this inhomogeneity is termed inhomogeneous broadening. If the fluctuations are much faster, the interaction can be seen as an interaction of the pigment with the phonons of the environment. This is called homogeneous broadening. Both broadening effects have a large effect on the spectroscopic properties of these complexes. Leegwater investigated the effect of the homogeneous broadening on the exciton delocalization.[12] He calculated the influence of the electron−phonon interaction on the exciton delocalization in the high-temperature limit ($kT \gg V$). In this model the main parameter determining the exciton delocalization is Γ/V, where Γ is the homogeneous line width. Taking $\Gamma/V = 1$, which is a reasonable assumption for these systems (vide infra), he estimates that in LH-1 the number of coherently coupled pigments is on the order of four pigments. This illustrates that electron−phonon coupling causes localization of the excitation on a small section of the ring. To examine the influence of site inhomogeneity on the excitonic behavior we have performed Monte Carlo simulations on such ringlike structures. From the results shown in Figures 3 and 4 one specific aspect of the ringlike structure is immediately clear, namely, that at $\sigma_{inh} = 0$ the lowest state is dipole forbidden and that disorder actually causes the superradiance in these systems. The interplay between the two effects of disorder, making the lowest state dipole allowed and breaking down the exciton delocalization, results in maximal amounts of superradiance that are significantly less than the aggregate size of these complexes (see Figures 3 and 4). The symmetry and size of these complexes thus set an absolute maximum limit for the superradiance regardless of the coupling strength and the inhomogeneity. These maxima are 4.2 and 7.6 for LH-2 (18 pigments) and LH-1 (32 pigments), respectively. We emphasize that the emitting dipole strength and the localization calculated this way give an *upper limit* to the true value. Additional effects, such as electron−phonon coupling and inclusion of vibrations, cause additional localization and thus a decrease of the superradiance.[12,21] However, recent calculations by Meier et al. showed that inclusion of phonons into the model does not markedly change the amount and temperature dependence of the superradiant emission.[42]

Parameters. In the model described above, the main parameter describing the superradiance is the ratio of the fwhm of the inhomogeneous distribution function and the coupling strength between the pigments (σ/V). One limit for the coupling strength can be extracted from the red-shift of the exciton band relative to the monomer transitions. For a ringlike aggregate without inhomogeneity this shift equals $2V$. Simulations on ringlike pigment organizations (not shown), J-aggregates,[21] and dimers[43] have indicated that the location of the long-wavelength exciton band is only weakly dependent on the amount of

inhomogeneity. Assuming that the monomer frequency is not shifted by the protein (so $\lambda_{mon} = 780$ nm), an absolute maximum coupling of 300 cm^{-1} for the B820 band of the B800-820 complex and 530 cm^{-1} for the B850 band of the B800-850 complex can be calculated. Since the spectroscopy of the 820 band in B800-820 and the 850 band in B800-850 is very similar, it seems most probable that the shift from 820 to 850 nm is due to a shift of the monomer frequencies instead of an increase in the coupling strength between the pigments. This argument suggests that $V < 300$ cm^{-1}. Moreover taking $\lambda_{mon} = 780$ nm probably underestimates the monomer wavelength. Van Mourik et al. could satisfactorily fit the T-S spectrum of the B820 subunit of LH-1 using a monomer frequency of 808 nm,[43] whereas Pearlstein found a best fit of the absorption and circular dichroism spectrum of the FMO complex of *Prosthecochloris aestuarii* using monomer transitions around 800 nm.[44] Using the point monopole approximation, Sauer et al.[11] calculated for the B850 ring of LH-2 a coupling between the pigments of 273 cm^{-1}, based on an ϵ_r of 2.1. This value was about 25% lower than a simple point dipole approximation. Thus, a reasonable assumption for the coupling strength between the pigments is between 200 and 300 cm^{-1}.

The static inhomogeneity of these antenna complexes has been probed with hole burning, steady-state fluorescence spectroscopy, and a variety of ultrafast time-resolved measurements.[13−15] Hole-burning measurements have shown that in the B800 band of LH-2, narrow holes can be burnt over the whole absorption band (at 4.2 K), suggesting that most of the width of this band (170 cm^{-1}) is due to inhomogeneous broadening.[15] From site-selected fluorescence measurements on the B820 subunit,[16] and spectral modeling of the absorption and fluorescence spectra,[45,46] it was concluded that the width of the inhomogeneous distribution function (IDF) of this subunit is approximately 250−350 cm^{-1}. From modeling of pump probe measurements an estimate of 400 cm^{-1} at room temperature and 200 cm^{-1} at 4 K for the LH-1 antenna of *Rs. rubrum* was made by Visser et al.[13,47] Leupold et al.[48] find that the B850 band of *Rb. sphaeroides* is heterogeneously broadened with four different pigment pools spanning a width of 600 cm^{-1}. Fluorescence upconversion measurements were modeled with an IDF of 250 cm^{-1} for both LH-1 and LH-2 of *Rb. sphaeroides*.[32,49] From a comparison of the values of the coupling and the inhomogeneity in these complexes, we conclude that the ratio of inhomogeneity to coupling in LH-1 and LH-2 of purple bacteria is in the range of $\sigma/V = 0.5-1.5$.

Comparison of Simulations and Measurements. There is strong evidence that the B820 subunit is a dimer of 2 Bchl-*a* molecules.[16] Modeling of the influence of the site inhomogeneity on the excitonic spectrum showed that the average dipole strength of the lowest excitonic state of the dimer is about 1.9 times the monomer value.[50] Weighing the exciton spectrum with a Bolzmann distribution using the same method as described above, we find that the average emitting dipole of such a dimer is 1.7 at room temperature with $\sigma/V = 1$, an angle of 20° between the monomers, and $V = 200$ cm^{-1} (not shown). This is somewhat larger than the observed value of 1.3. However, as mentioned above, an additional localization of the excitation can be caused by interactions with phonons,[12] which could explain the difference between the observed and calculated superradiance. From our measurements of the room temperature and temperature-dependent radiative rate, we find distinct differences between LH-1 and LH-2. In LH-2 the room temperature value of the dipole strength is about 2.8 times the monomer value. This value agrees well with the simulations shown in Figure 4, if we assume a coupling of 200 cm^{-1} and $\sigma/V > 1$. The emitting dipole strength is actually quite insensitive for the inhomogeneity at room temperature. There is however a strong dependence of the shape of the temperature dependence on the amount of inhomogeneity. LH-2 shows very little temperature dependence which would in fact correspond with an inhomogeneity to coupling ratio of $\sigma/V = 2$ or higher.

For the LH-1 complex we observe a totally different behavior. As for the ring consisting of 18 pigments, calculations show that the emitting dipole strength at high temperature is only weakly dependent on the amount of inhomogeneity (not shown). For $\sigma/V = 1$ and $V = 200$ cm^{-1}, we calculate an emitting dipole strength of 3 at room temperature, which is somewhat lower than the experimentally observed superradiance (3.8). The experimentally observed dependence of the emitting dipole strength on temperature is much stronger in LH-1 than in LH-2. To reproduce the observed temperature dependence, we need to take a low value for σ/V. Taking σ/V equal to 1, the model predicts a maximal increase of superradiance of 2.1 at 4 K relative to room temperature (see Figure 4). This is close to the experimentally observed increase of 2.4, and also the rise with temperature is smooth as observed in the experiment. However, for these values of the parameters the calculated emitting dipole strength is significantly lower than the measured amount of superradiance. We note that, within our model, the maximum superradiance is limited by the size of the ring. Even for $\sigma/V = 0$, the maximum superradiance in a ring consisting of 32 monomers is 7, which is smaller than the value obtained by multiplying the measured room temperature radiative rate and the temperature-dependent rise. One explanation for the high superradiance could be that the structure is not ringlike. However electron microscopy measurements on an identically prepared sample have shown that the sample mainly consists of small isolated rings.[22] As was stated above, to calculate the absolute amount of superradiance (or emitting dipole strength) from the radiative rate, both the refractive index of the medium and the relative dielectric constant of the protein need to be known. The experimentally obtained higher value of the emitting dipole strength at room temperature for LH-1 could indicate that the dielectric constant in this complex is somewhat lower. For instance a dielectric constant of 1.85 would bring the measured value in agreement with the simulation shown in Figure 4. Furthermore in our simulations we have taken both V and σ to be temperature independent. Visser et al.[13,42] estimated for LH-1 of *Rb. sphaeroides* an inhomogeneous broadening of 200 cm^{-1} at 4 K and 400 cm^{-1} at room temperature. This suggests that for LH-1 the inhomogeneity could be temperature dependent. This observation is supported by the temperature-dependent absorption spectra of the LH-1 and LH-2 complexes of *Rb. sphaeroides*. The B850 band of the LH-2 complex does not shift between room temperature and 4 K and only slightly narrows (25%). The B880 band of the LH-1 complex however shifts approximately 11 nm to the red and narrows considerably (55%), indicating a strong temperature dependence of the inhomogeneous broadening in LH-1. Narrowing of the IDF causes a lower value of σ/V and could thus cause a higher superradiance. It is thus very likely that, in LH-1, the temperature dependent increase of the radiative rate is due to both a decrease of the inhomogeneity and the thermal population of higher lying exciton states. Also, the coupling could depend on temperature. Shrinking of the protein can for instance make intermolecular distances smaller and thus enlarge the coupling. However, from an analysis of the CD spectrum at room temperature and at 4 K, we have recently concluded that the coupling (as reflected by the rotational strength of the excitonic transitions) does not change markedly.[51]

Localization. To examine the localization of the excitations within the LH-1 and LH-2 complex, we have looked at the squared wave functions of the exciton states that carry dipole strength. This distribution shows the contribution of the excited state of each pigments to the collective exciton state. As can be seen from Figure 5, already a small amount of inhomogeneity causes the exciton to be localized on a limited number of pigments. Several groups have tried to estimate the amount of localization using different methods. One frequently used measure for the amount of pigments that participate in the excitonic state is the so-called participation ratio.[21] It is however not clear how the participation ratio relates to the average number of pigments that contribute to a certain excitonic transition. Our simulations show that, for an LH-2-like structure with $\sigma/V = 1$, the average participation ratio is equal to 8.3. From the average wave function that is calculated using the same parameters (see Figure 5), it is however clear that the exciton is distributed over a much smaller number of pigments. Both the second moment and the fwhm of the distribution are significantly smaller than the participation ratio (5.4 and 2.6 pigments, respectively).

Unfortunately in other than linear aggregates, the observable superradiance is not easily related to the delocalization length since the emitting (lowest) state does not have to be the exciton state where all the oscillator strength is concentrated. The amount of superradiance however sets a lower limit to the number of pigments participating in the emitting state. From this we conclude that the delocalization in LH-1 and LH-2 is, at room temperature, at least 3−4 pigments. However, from our point of view, a visual description of the exciton delocalization, as for instance shown in Figure 5 or as presented by Meier et al.,[43] gives a more meaningful description than a single quantity.

V. Summary

In this work we have measured the superradiance of the B820 subunit of *Rs. rubrum* and the LH-1 and LH-2 complexes of *Rb. sphaeroides*. We find that, at all temperatures, the dipole strength of the emitting state is higher than that of monomeric Bchl-*a*, indicating the presence of collective excitations in these antenna systems. B820 shows only a small increase of the dipole strength, in agreement with a dimeric model for this subunit. The LH-1 and LH-2 complexes have, at room temperature, an emitting dipole strength that is 3.8 and 2.8 times that of monomeric Bchl-*a*, respectively, using a value of 2.3 for the relative dielectric constant of the protein. The measured superradiance of the LH-1 complex is larger than expected, which could be due to a lower dielectric constant in this antenna complex. The temperature dependence of the superradiance is surprisingly different between LH-1 and LH-2 of *Rb. sphaeroides*. Whereas the radiative rate of LH-2 remains constant, the radiative rate of LH-1 increases a factor of 2.3 going from room temperature to 4 K. The weak temperature dependence of the radiative rate in LH-2 is probably indicative of a relatively large value of σ/V in this complex ($\sigma/V = 2-3$), together with a weak dependence of inhomogeneity on temperature. The temperature dependence of the LH-1 complex is most likely due to a combination of a temperature-dependent narrowing of the inhomogeneous distribution function, and a relatively low value of around 1 for σ/V. Simulations of the influence of site inhomogeneity on the excitonic spectrum of circular aggregates show that some of the spectral properties are strongly dependent on inhomogeneity. Analyzing the average wave functions of the excitonic states within our model, we find that the inhomogeneity causes a strong localization of the excitation on a part of the ring.

Acknowledgment. The authors acknowledge Ing. F. Calkoen and Ing. H. van Roon for the preparation and purification of the light-harvesting complexes. Furthermore, we thank Dr. I. H. M. van Stokkum for assistance with the analysis of the time-resolved fluorescence measurements. M.A. was supported by a grant from the European Union in the framework of the Erasmus program. This research was supported by grants from The Netherlands Organization for Scientific Research (NWO) via the foundation of Life Sciences (SLW), the E.U. contract 93-0278, and the "Human Frontiers in Science" program.

References and Notes

(1) van Grondelle, R.; Dekker: J. P.; Gillbro, T.; Sundström, V. *Biochim. Biophys. Acta* **1994**, *1187*, 1.

(2) Monshouwer, R.; van Grondelle, R. *Biochim. Biophys. Acta* **1996**, *1275*, 70.

(3) McDermott, G.; Prince, S. M.; Freer, A. A.; Hawthornthwaite-Lawless, A. M.; Papiz, M. A.; Cogdell, R. J.; Isaacs, N. W. *Nature* **1995**, *374*, 517.

(4) Freer, A. A.; Prince, S.; Sauer, K.; Papiz, M.; Hawthornthwaite-Lawless, A.; McDermott, G.; Cogdell, R. J.; Isaacs, N. W. *Structure*, **1996**, *4*, 449.

(5) Koepke, J.; Xiche, H.; Muenke, C.; Schulten, K.; Michel, H. *Structure* **1996**, *4*, 581.

(6) Karrasch, S.; Bullough, P. A.; Ghosh, R. *EMBO J.* **1995**, *14* (4), 631.

(7) Novoderezhkin, V. I.; Razjivin, A. P. *FEBS Lett.* **1993**, *330*, 5.

(8) Pullerits, T.; Chachisvilis, M.; Sundström, V. *J. Phys. Chem.* **1996**, *100*, 10787.

(9) Sturgis, J. N.; Robert, B. *Photosynth. Res.* **1996**, *50*, 5.

(10) Koolhaas, M. H. C.; van der Zwan, G.; van Mourik, F.; van Grondelle, R. Submitted for publication in *J. Phys. Chem.*

(11) Sauer, K.; Cogdell, R. J.; Prince, S. M.; Freer, A. A.; Isaacs, N. W.; Scheer, H. *Photochem. Photobiol.* **1996**, *64*, 3, 564.

(12) Leegwater, J. A. *J. Phys. Chem.* **1996**, *100*, 14403.

(13) Visser, H. M.; Somsen, O. J. G.; van Mourik, F.; Lin, S.; van Stokkum, I. H. M.; van Grondelle, R. *Biophys. J.* **1995**, *69*, 1083.

(14) Jimenez, R.; van Mourik, F.; Fleming, G. R. Submitted for publication in *J. Phys. Chem.*

(15) Reddy, N. R. S.; Small, G. J.; Seibert, M.; Picorel, R. *Chem. Phys. Lett.* **1991**, *181* (5), 391.

(16) Visschers, R. W.; van Mourik, F.; Monshouwer, R.; van Grondelle, R. *Biochim. Biophys. Acta* **1993**, *1141*, 238.

(17) van Mourik, F.; Visschers, R. W.; van Grondelle, R. *Chem. Phys. Lett.* **1992**, *195*, 1.

(18) Scheibe, G. *Angew. Chem.* **1936**, *49*, 563.

(19) Jelley, E. E. *Nature* **1936**, *138*, 1009.

(20) Fidder, H.; Wiersma, D. A. *Phys. Rev. Lett.* **1991**, *66* (11), 1501.

(21) Fidder, H.; Knoester, J.; Wiersma, D. A. *J. Chem. Phys.* **1991**, *95*, 7880.

(22) Boonstra, A. F.; Visschers, R. W.; Calkoen, F.; van Grondelle, R.; van Bruggen, E. F. H.; Boekema, E. J. *Biochim. Biophys. Acta* **1993**, *1142*, 181.

(23) Hunter, C. N.; Bergström, H.; van Grondelle, R.; Sundström, V. *Biochemistry* **1990**, *29*, 3203.

(24) Miller, J. F.; Hinchigeri, S. B.; Parkes-Loach, P. S.; Callahan, P. M.; Sprinkle, J. R.; Loach, P. A. *Biochemistry* **1987**, *26*, 5055.

(25) Monshouwer, R.; Ortiz de Zarate, I.; van Mourik, F.; van Grondelle, R. *Chem. Phys. Lett.* **1995**, *246*, 341.

(26) Connolly, J. S.; Samuel, E. B.; Janzen, A. F. *Photochem. Photobiol.* **1982**, *36*, 565.

(27) Timpmann, K.; Freiberg, A.; Godik, V. I. *Chem. Phys. Lett.* **1991**, *182* (6), 617.

(28) Moog, R. S.; Kuki, A.; Fayer, M. D.; Boxer, S. G. *Biochemistry* **1984**, *23*, 1564.

(29) This is different from dipole strengths used by others.[8,9,11] Note however that this is the dipole strength in vacuum. Many authors use the vacuum dipole strength divided by the relative dielectric constant of the medium in which the dipole strength has been determined. Using n=1.36 for acetone and $|\mu|^2 = 68$ D^2, we find for $|\mu|^2/\epsilon_r$ a value of 38.5 D^2.

(30) Renge, I.; van Grondelle, R.; Dekker: J. P. *Photochem. Photobiol.* **1996**, *96*, 109.

(31) Andersson, P. O.; Gillbro, T.; Ferguson, L.; Cogdell, R. J. *Photochem. Photobiol.* **1991**, *54*, 353.

(32) Jimenez, R.; Dikshit, S. N.; Bradforth, S. E.; Fleming, G. R. *J. Phys. Chem.* **1996**, *100*, 6825.

(33) Press: W. H.; Flannery, B. P.; Teukolsky, S. A.; Vettering, W. T. *Numerical Recipes*; Cambridge University Press: Cambridge, 1987.

(34) Pearlstein, R. M. In *Chlorophylls*; Sheer, H., Ed.; CRC Press: Boca Raton, FL, 1991; p 1047.
(35) Wu, H. M.; Reddy, N. R. S.; Small, G. J. *J. Phys. Chem.* **1997**, *101*, 651.
(36) Chachisvilis, M.; Pullerits, T.; Westerhuis, W.; Hunter, C. N.; Sundström, V. Submitted for publication in *J. Phys. Chem.*
(37) Schreiber, M.; Toyozawa, Y. *J. Phys. Soc. Jpn.* **1982**, *51* (5), 1537.
(38) de Boer, S.; Wiersma, D. A. *Chem. Phys. Lett.* **1990**, *165* (1), 45.
(39) Kramer, H. J. M.; van Grondelle, R.; Hunter, C. N.; Westerhuis, W. H. J.; Amesz, J. *Biochim. Biophys. Acta* **1984**, *765*, 156.
(40) van Amerongen, H.; van Haeringen, B.; van Gurp, M.; van Grondelle, R. *Biophys. J.* **1991**, *59*, 992.
(41) Fowler, G. J. S.; Visschers, R. W.; Grief, G. G.; van Grondelle, R.; Hunter, C. N. *Nature* **1992**, *355*, 848.
(42) Meier, T.; Chernyak, V.; Mukamel, S. Submitted for publication in *J. Phys. Chem.*
(43) van Mourik, F.; van der Oord, C. J. R.; Visscher, K. J.; Parkes-Loach, P. S.; Loach, P. A.; Visschers, R. W.; van Grondelle, R. *Biochim. Biophys. Acta* **1991**, *1059*, 111.
(44) Pearlstein, R. M. *Photosynth. Res.* **1992**, 31, 213.
(45) Pullerits, T.; van Mourik, F.; Monshouwer, R.; Visschers, R. W.; van Grondelle, R. *J. Lumin.* **1994**, *58*, 168.
(46) Pullerits, T.; Monshouwer, R.; van Mourik, F.; van Grondelle, R. *Chem. Phys.* **1995**, *194*, 395.
(47) Visser, H. M.; Somsen, O. J. G.; van Mourik, F.; van Grondelle, R. *J. Phys. Chem.* **1996**, *100*, 18859.
(48) Leupold, D.; Voigt, B.; Nowak, F.; Ehlert, J.; Hirsch, J.; Neef, E.; Bandilla, M.; Scheer, H. *Liet. Fiz. Zur.* **1994**, *34*, 339.
(49) Bradforth, S. E.; Jimenez, R.; van Mourik, F.; van Grondelle, R.; Fleming, G. R. *J. Phys. Chem.* **1995**, *99*, 16179.
(50) Koolhaas, M. H. C.; van Mourik, F.; van der Zwan, G.; van Grondelle, R. *J. Lumin.* **1994**, *60*/*61*, 515.
(51) Somsen, O. J. G. Personal communication.